Spin Seebeck coefficient and spin-thermal diffusion in the two-dimensional Hubbard model

Jernej Mravlje[1], Martin Ulaga[1] and Jure Kokalj[2,1]
[1]*Jozef Stefan Institute, Jamova 39, Ljubljana, Slovenia*
[2]*University of Ljubljana, Faculty of Civil and Geodetic Engineering, Jamova 2, Ljubljana, Slovenia*

(Received 4 August 2021; revised 4 March 2022; accepted 7 March 2022; published 7 June 2022)

We investigate the spin Seebeck coefficient S_s in the square lattice Hubbard model at high temperatures of relevance to cold-atom measurements. We solve the model with the finite-temperature Lanczos and with the dynamical mean-field theory methods and find they give similar results in the considered regime. S_s exceeds the atomic Heikes' estimates and the Kelvin entropic estimates drastically. We analyze the behavior in terms of a mapping onto the problem of a doped attractive model and derive an approximate expression that allows relating the enhancement of S_s to distinct scattering of the spin-majority and the spin-minority excitations. Our analysis reveals the limitations of entropic interpretations of Seebeck coefficient even in the high-temperature regime. Large values of S_s could be observed on optical lattices. We also calculated the full diffusion matrix. We quantified the spin-thermal diffusion, that is, the extent of the mixing between the spin and the thermal diffusion and discuss the results in the context of recent measurements of the spin-diffusion constant in cold atoms.

DOI: 10.1103/PhysRevResearch.4.023197

I. INTRODUCTION

Cold-atom systems on optical lattices provide a novel lens on poorly understood transport regimes of correlated electrons [1,2]. The cold atoms can realize the Hubbard model—the standard model of correlated electrons that interact with an on-site repulsion U and move on the lattice (hopping t)—without real world complications, such as lattice vibrations and disorder. Hence one can directly and quantitatively compare the outcome of the experiment with those of the numerical solutions of the Hubbard model [1,2]. Such a cross-verification turned very successful in the measurements of the charge diffusivity [1]. Besides providing an important mutual benchmark of the methods it led to a quantification of the vertex corrections [3]. Intriguingly, related measurements of spin diffusivity revealed a disagreement between the numerical methods and the experiment [2]. An independent numerical investigation [4] confirmed the results of the theory but disagreed with the experiment.

This disagreement thus calls for a close inspection of the underlying assumptions of the experimental analysis. One of the assumptions is that the spin-thermoelectric effect is unimportant. This holds strictly at a vanishing magnetization, but in the actual experiment this condition was only approximately met as some spin imbalance $m_z = (n_\uparrow - n_\downarrow)/2$ is seen in the measurements: $|m_z| \lesssim 0.05$ [2]. The strength of the spin-thermoelectric effect is quantified by the spin Seebeck coefficient S_s given by the ratio of the magnetic field and thermal gradient at the condition of vanishing spin current, $S_s = \nabla B/\nabla T|_{j_s=0}$. S_s is a quantity that is relevant for spintronics applications [5–8] but has to our knowledge not been discussed for the Hubbard model (surprisingly, as this is the paradigmatic model of correlated electrons). The intention of our work is to fill this gap, establish how large S_s is in the high-temperature regime, and use that knowledge to discuss whether the measurements of spin-diffusion in cold atoms could be influenced by the spin-thermoelectric effects.

Some intuition concerning S_s could be expected from considerations that relate the ordinary charge Seebeck coefficient S_c to thermodynamic quantities, such as the high-temperature Heikes limit $S^H = \mu/T$ or the Kelvin formula $S^K = d\mu/dT$ that relate the Seebeck coefficient to the temperature dependence of the chemical potential [9–12]. Namely, it was demonstrated that often at high temperatures the Kelvin formula describes the Seebeck coefficient well [11] (but some exceptions to this were also noted [13]).

To apply this intuition to S_s one can use a mapping that relates the spin transport in a magnetized repulsive Hubbard model to the charge transport in a doped attractive Hubbard model [14–21]. This mapping proceeds via a particle-hole transformation on particles of only one spin, e.g., $\downarrow$, with $c_{i,\downarrow} \to (-1)^i c^\dagger_{i,\downarrow}$ and results in an interchange of spin and charge degrees of freedom, explicitly $n_\uparrow - n_\downarrow \to n_\uparrow + n_\downarrow$, $n_\uparrow n_\downarrow \to -n_\uparrow n_\downarrow$. Accordingly, Hubbard repulsion goes to attraction, $Un_\uparrow n_\downarrow \to -Un_\uparrow n_\downarrow$. Via this mapping, one can relate the spin Heikes estimate for spin Seebeck coefficient $S_s^H = B/T|_{m_z=\text{const}}$ (or Kelvin estimate $S_s^K = dB/dT|_{m_z=\text{const}}$) to the corresponding charge Heikes and Kelvin estimates for a model with an opposite sign of repulsion (that is, an attractive model for the case of interest here). Actually, by exploiting the mapping one can use the results from the literature [22] and obtain $S_s = 8k_B m_z$ at a high-temperature ($T > U$) and $S_s = 4k_B m_z$ at a lower temperature ($T < U$).

From these estimates—that one is inclined to trust, especially in the high-temperature regime $T > t$ pertinent to cold-atom measurements—one expects only small values of the spin Seebeck coefficient $S_s \ll k_B$, since $m_z \ll 1$.

In this paper we show that this reasoning is incorrect. We calculate S_s for a square lattice Hubbard model at high T using the finite temperature Lanczos method (FTLM) and the dynamical mean-field theory (DMFT) approaches and find that it strongly exceeds the bounds just discussed. S_s violates the thermodynamic expectations even in the high-temperature regime, an unexpected finding based on what was previously known for the ordinary thermoelectric effect. Large values of S_s call for a reexamination of the possible spin-thermoelectric effects in cold-atom measurements of spin diffusion. To estimate those, we calculated the full diffusion matrix $\mathbf{D}$. In general, the eigenvalues of $\mathbf{D}$ deviate from those found in the absence of spin-thermoelectric effect. Interestingly, we find the deviations are related to the difference between the actual value of spin Seebeck coefficient and its thermodynamic Kelvin approximate, $S_s - S_s^K$. We discuss why in spite of this difference being sizable (it exceeds k_B at large U) the final influence on the measured spin diffusion for moderate magnetization is unimportant.

We note that large values of Seebeck coefficient for the attractive model were earlier found in the DMFT [21] but were not compared with the thermodynamic estimates and the importance of those results for the spin-thermoelectric response was not discussed.

The remainder of the paper is structured as follows. In Sec. II we specify the model, the methods, and the notation. In Sec. III we show our main results for the spin Seebeck coefficient. In Sec. IV we describe the DMFT calculation of transport and in Sec. V we exploit it in conjunction with the mapping to an attractive model to interpret our results. In Sec. VI we investigate the influence of the spin-thermoelectric effect for the spin diffusion. In Sec. VII we give our conclusions. The Appendix discusses the behavior of spin Seebeck coefficient for a phenomenological ansatz spectral function.

II. MODEL AND METHOD

We study the square lattice Hubbard model,

$$H = -t \sum_{\langle i,j\rangle, s=\uparrow,\downarrow} c^{\dagger}_{i,s} c_{j,s} + U \sum_i n_{i,\uparrow} n_{i,\downarrow}, \tag{1}$$

with t being the hopping between the nearest neighbors. We take $\hbar = k_B = e = g\mu_B = 1$. We likewise take lattice spacing $a = 1$. We use t as the energy unit.

We solve the Hamiltonian with FTLM [23–25] on a $N = 4 \times 4$ cluster and in the thermodynamic limit with the DMFT [26] [that is, we solve the Hamiltonian Eq. (1) in a local approximation]. The DMFT equations are solved using the numerical-renormalization group (NRG) [27] in the NRG-Ljubljana implementation [28] as the impurity solver.

III. SPIN SEEBECK COEFFICIENT

Figure 1(a) displays S_s as a function of temperature for $U = 10$ evaluated with the FTLM (full, thick) and the DMFT (symbols). At highest temperatures, S_s approaches the high-temperature Heikes value, $2\log(1+2m_z)/(1-2m_z) \approx 8m_z$, which is the expected behavior. The Kelvin estimate from $dB/dT|_{m_z}$ evaluated using the FTLM (thin; DMFT gives similar results) agrees with the Kubo evaluation in this regime. On lowering the temperature, surprisingly, instead of diminishing in amplitude as suggested by the Heikes value corresponding to $T < U$, $\log[(1+2m_z)/(1-2m_z)] \approx 4m_z$ [22], S_s increases and reaches a maximum value well above the Heikes estimate and only drops consequently at lower T. This behavior with a substantial increase of the spin-thermoelectric coefficient above the high-temperature and thermodynamic estimates becomes even more pronounced for larger U, as displayed in Fig. 1(b). The magnitude of the peak diminishes with decreasing magnetization but increases with increasing U. It is, as we show below, proportional to $m_z U/T$.

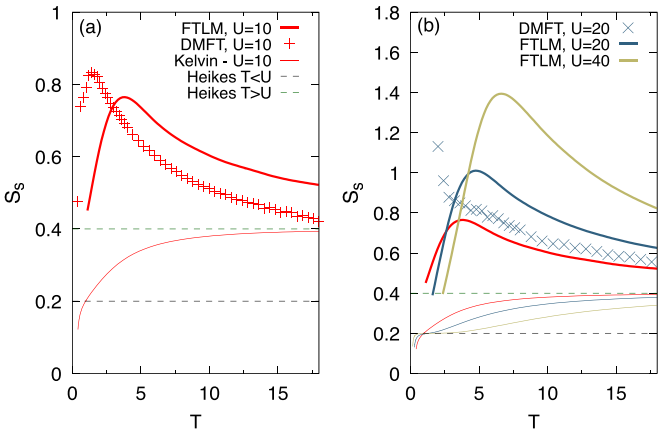

FIG. 1. (a) The spin Seebeck coefficient for $U = 10$ at half filling for magnetization $m_z = 0.05$, calculated using the FTLM (thick) and the DMFT (+). Kelvin estimates (thin) and the two Heikes' estimates are also shown (dashed). (b) The FTLM data for $U = 10, 20, 40$ (thick) along the Kelvin estimates (thin). The DMFT data for $U = 20$ are also shown (crosses).

Throughout the considered regime, the temperatures are high ($T > t$) and one cannot attribute the deviations from the thermodynamic estimates to the occurrence of coherent transport or to a proximity to a magnetically ordered regime. The observed deviations are in stark contrast to the behavior of the charge thermopower that at temperatures $T > t$ does follow the thermodynamic estimates [11].

IV. DMFT DESCRIPTION OF TRANSPORT

In order to understand this behavior it is convenient to discuss the transport properties within the DMFT approach. The DMFT expresses the transport coefficients in terms of the transport function [29]

$$\Phi_\sigma(\omega) = \sum_k v_k^2 A_{k\sigma}^2(\omega), \tag{2}$$

where v_k is the band velocity: $v_k = d\epsilon/dk_x$ with ϵ_k the band energy. $A_{k\sigma}$ is the spectral function at momentum k and spin σ. The charge Seebeck S_c and the spin Seebeck S_s coefficients

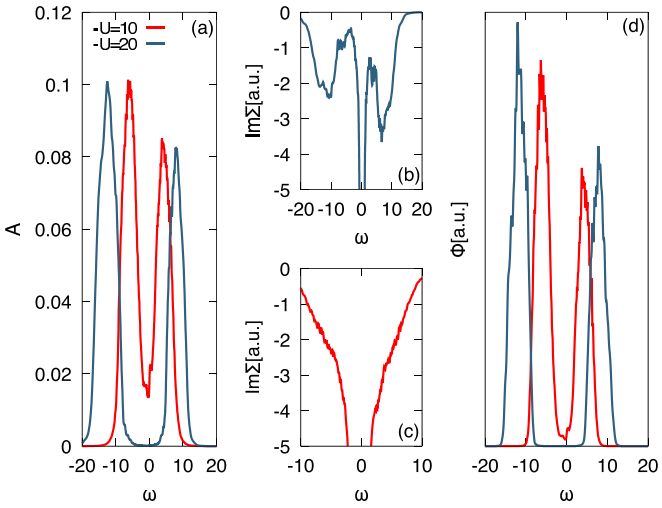

FIG. 2. (a) The DMFT spectral function $A(\omega)$ for the doped attractive model $\delta = n - 1 = 0.1$ (corresponding to $m_z = 0.05$) for $-U = 10, 20$ at temperature $T = 6$. (b), (c) The corresponding imaginary part of the self-energy, and (d) the DMFT transport function $\Phi(\omega)$.

are, respectively,

$$S_{(s,c)} = (1, 2)\frac{\int(\Phi_\uparrow(\omega) \pm \Phi_\downarrow(\omega))(-\omega/T)(-df/d\omega)d\omega}{\int(\Phi_\uparrow(\omega) + \Phi_\downarrow(\omega))(-df/d\omega)d\omega}. \tag{3}$$

As seen in Fig. 1(a), the DMFT results are similar although not identical to the FTLM ones. To what extent the differences are technical (it is quite challenging to converge the DMFT calculations in this regime as discussed in Ref. [21]) or physical, such as emanating in nonlocal fluctuations and/or the vertex corrections neglected in DMFT, is a question that goes beyond the scope of the present paper. It is likely that at low T the vertex corrections become more important as the DMFT calculation gives an insulator with a spin gap whereas the actual behavior is that of a spin conductor described by a Heisenberg model. For our purpose we will ignore these differences between the two methods and exploit the more transparent DMFT formulation of transport to interpret the FTLM results.

V. MAPPING TO THE ATTRACTIVE MODEL

It is convenient to analyze the results in terms of the mapping of the spin to the charge degrees of freedom for an attractive model, that is $S_s(U) = 2S_c(-U)$, with the spin polarization $2m_z \to \delta$ becoming the charge doping with factors of 2 occurring due to the definition of spin.

Figure 2(a) presents the local spectral function $\sum_k A_k(\omega)$ of the doped attractive model at $T = 6$, for two values of attraction $-U = 10, 20$. As discussed in earlier studies of the attractive model [16,17,21,30], the spectral function consists of two peaks, which are as for the repulsive Hubbard model centered at $-\mu$ and $-\mu + U$, with $\mu \sim U/2$. The important distinction between the doped attractive and the doped repulsive model is in the behavior of the chemical potential with temperature that can at high T be most simply obtained from a grand-canonical treatment of the atomic problem. There, average electron occupancy can be evaluated from

$$n = \frac{2\exp(\beta\mu) + 2\exp(-\beta(U - 2\mu))}{1 + 2\exp(\beta\mu) + \exp(-\beta(U - 2\mu))}. \tag{4}$$

In the attractive model, terms that include $\exp(-\beta U)$ grow at low temperatures and should be retained. Hence one obtains

$$\mu = U/2 + \delta\mu = U/2 + T\log((1 + \delta)/(1 - \delta)). \tag{5}$$

The fact that $\mu \sim U/2$ at low T represents a crucial difference with respect to the repulsive case causes the spectral function to be gapped at a nonvanishing doping. Namely, the spectral function consists of two peaks displaced by $\delta\mu$ from $\pm U/2$ as shown on Fig. 2(a) for two values of U. Because at large $|U|$ the gap is well developed, the lower and upper Hubbard bands must have unequal spectral weight to yield a finite doping.

Figure 2(d) presents the transport function. One sees that this exhibits the two Hubbard bands and is overall similar to the density of states. There is, however, an important difference: Because Φ contains A_k^2, the weights of the upper and the lower Hubbard band parts are affected by the amplitude of scattering, as given by self-energy depicted in Figs. 2(b) and 2(c) for $|U| = 20, 10$, respectively. When the spectral function is a sharply peaked function, $A_k^2 \sim A_k/(2\pi\Gamma_k)$ with $\Gamma_k = -\mathrm{Im}\Sigma(\omega_k)$, and hence the transport function is modulated by the value of the self-energy at the peak frequency ω_k. In passing we note that this finding can be used to connect the bubble expression to the Boltzmann calculation, see Refs. [31,32] for a recent discussion.

In the Appendix we take advantage of the simple two-peaked structure of the transport function and find an expression

$$S_c = -\frac{U}{2T}\frac{\tilde{\phi}_- - \tilde{\phi}_+}{\tilde{\phi}_- + \tilde{\phi}_+} + \frac{\delta\mu}{T} = S_1 + \frac{\delta\mu}{T}, \tag{6}$$

where the first term grows as U/T and is proportional to a coefficient that is expressed in terms of the effective weights of the positive (negative) frequency peaks of the transport function $\tilde{\phi}_\pm$. This coefficient (that is found to be approximately given by doping; see the Appendix) grows with the difference in the scattering between the holes and the electrons. When this difference does not vanish, the behavior of the Seebeck coefficient differs from that of the thermodynamic expectations given by the second term in Eq. (6).

Let us relate this discussion to the repulsive case. At the particle-hole symmetry, the spectral functions of the repulsive and attractive case for, respectively, $s = \uparrow, \downarrow$ are related by $A_{k\uparrow,\downarrow}(\omega)|_{U>0} = A_{k\uparrow,\downarrow}(\pm\omega)|_{U<0}$. That is, taking advantage of the mapping, Fig. 2 depicts $s = \uparrow$ components of the spectral function, the self-energy, and the transport function, and the $s = \downarrow$ components can be obtained by $\omega \to -\omega$. The different scattering between the electrons and the holes in the attractive model thus relates to a different scattering between the spin majority and the spin-minority carriers in the repulsive model, and this in turn leads to $S_s \sim m_z U/T$ behavior that explains the enhancement over the thermodynamic estimates seen in Fig. 1.

VI. DIFFUSION MATRIX, DIFFUSION EIGENVALUES, AND RELEVANCE FOR EXPERIMENT

Predicted large values of spin Seebeck coefficient at large T and the increase of the peak value with increasing U (or the corresponding behavior of the charge-Seebeck coefficient in the attractive case) could be tested in future cold-atom experiments. In the introduction we also raised a possibility that the existing measurements of spin diffusion would be affected by spin-thermoelectric effects, which could account for values of the spin diffusion and the spin conductivity that were found to be larger than theoretically expected.

Let us try to estimate the influence of thermoelectric effects on spin conductivity using a hand-waving argument. At finite magnetization, gradients of magnetic field are accompanied by a gradient of energy and, assuming thermalization, a gradient of temperature, $\nabla T \sim \nabla E/c = m_z \nabla B/c$ with c as the specific heat. Temperature gradients drive the spin current via the spin-thermoelectric effect. Writing the spin current as $j_s = -L_{ss}\nabla B - L_{sq}\nabla T/T$, one has $j_s = -L_{ss}(1 - S_s m_z/c)\nabla B$. At $T \approx 3$ (relevant to experiment [2]), the values of specific heat are of the order $0.3k_B$; hence the correction of the estimated spin conductivity due to spin thermoelectricity for magnetization 0.05 where $S_s \approx 0.8$ would be at the 15% level. Importantly, because S_s and m_z are of equal sign, this estimate anticipates that the spin conductivity is actually reduced compared with the case where spin thermoelectricity is neglected.

In order to make this discussion more precise, one must consider a generalization of the Nernst-Einstein relation to a matrix formulation allowing for a mixed response [33], where the off-diagonal entries involve the mixed transport coefficient L_{sq} and the thermoelectric susceptibility $\xi = -\partial^2 f/\partial B \partial T$ where f is the free-energy density. The diffusion constant in matrix form reads $\mathbf{D} = -\mathbf{L}\mathbf{A}^{-1}$, where $\{j_q, j_s\} = \mathbf{L}\{\nabla T, \nabla B\}$ defines the conductivity matrix $\mathbf{L}$ and the heat-magnetization susceptibility matrix $\mathbf{A}$ is defined by $\{T\nabla s, \nabla m_z\} = \mathbf{A}\{\nabla T, \nabla B\}$ [34]. The diffusion eigenmodes that are involved in general nonvanishing spin and heat components are obtained by diagonalizing the matrix $\mathbf{D}$. We denote the diffusion eigenvalue whose mode contains a predominantly spin (heat) component by D_- (D_+), respectively. These are shown in Fig. 3(a) as a function of temperature for $U = 10, m_z = 0.05$ and are compared to the bare spin-diffusion constant $D_s = \sigma_s/\chi_s$ and bare heat diffusion constant $D_q = \kappa/c$, where we use term "bare" to indicate that the spin-thermal mixing is neglected.

One sees that, consistent with the hand-waving discussion above, the influence of the spin-thermoelectric effects is only moderate; the diffusion eigenvalues are close to the values obtained when there is no mixing. The behavior of $D_\mp$ being smaller (larger) than the corresponding bare diffusion is that of level repulsion.

The relatively small admixing occurs because the geometric mean of the off-diagonal elements $\sqrt{D_{sq}D_{qs}}$ is significantly smaller ($\lesssim 10\%$) than $D_{qq} - D_{ss}$. When any of the off-diagonal elements vanish, the spin-thermoelectric effect on diffusion vanishes. We inspect more closely D_{sq}. It can be rewritten as $D_{sq} = -D_s(\frac{\xi + S_s\chi_s}{c})$, which expresses *spin-thermal diffusion*, i.e., spin-thermoelectric mixing between the spin and the thermal diffusion. Note that S_s is multiplied by χ_s/c, which becomes large at $T \to 0$. This hints at a rich behavior at low temperatures and should be explored in future work. Using the Kelvin formula $S_s^K = dB/dT|_{m_z}$, one can further rewrite $D_{sq} = -D_s\frac{\chi_s}{c}(S_s - S_s^K)$. Interestingly, when the spin thermoelectricity or spin Seebeck coefficient is given by the Kelvin estimate, $D_{sq} = 0$, which leads to D_- and D_+ being respectively equal to D_{ss} and D_{qq}. In this case the spin modulation decays with pure spin diffusion constant $D_{ss} = \sigma_s/\chi_s$ and has an admixed thermal (heat) component. An initial spin modulation therefore also induces heat currents. On contrary, D_+ corresponds to pure heat diffusion decaying with the bare heat diffusion constant $D_{qq} = \kappa/c$.

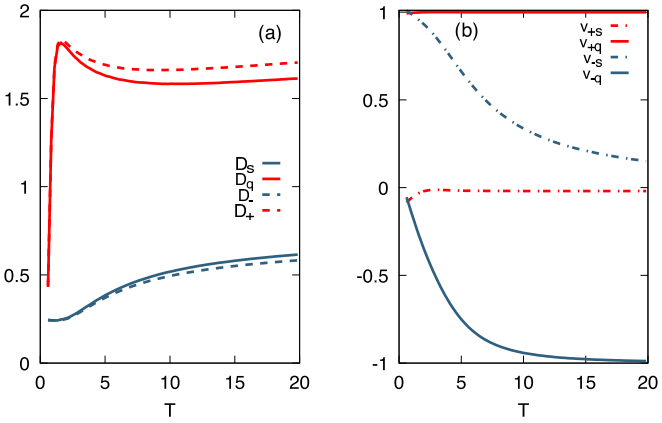

FIG. 3. (a) Bare spin-diffusion constant D_s, bare heat diffusion constant D_q, and the two eigenvalues of diffusion matrix $\mathbf{D}$ for $U = 10$ and magnetization $m_z = 0.05$. (b) Spin and heat components of eigenmodes $\vec{v}_\pm$ at $m_z = 0.05$

In experiment, an initial gradient of magnetization is imposed. Could larger values of the experimentally inferred spin-diffusion constant occur because there is a significant contribution of the heat eigenmode in the initial state that decays faster (see larger values of D_q and D_+ in Fig. 3)? The components of eigenvectors $\vec{v}_\pm$ are shown on Fig. 3(b). At $T = 3.1$ we find the spin-dominated eigenvector $\vec{v}_- = \{-0.53t, 0.84\}$, i.e., it contains a significant component of heat current that only increases with temperature. (In this expression we reintroduced t to indicate that the two components of $\vec{v}$ are in different units; because t is a natural unit for the energy, it is meaningful to compare the numerical values of the two components setting $t = 1$.) At the same temperature, the heat-dominated $\vec{v}_+ = \{0.999t, -0.02\}$ is mostly single component. One can first assume that the initial state is given by a pure magnetization gradient. Expanding this profile in terms of $\vec{v}_\pm$ we find only a small part of magnetization is contained in $\vec{v}_+$. To be specific, at $T = 3.1$, $\vec{v}_+$ contains $\sim 2\%$ of the initial spin modulation (the relative weight of $\vec{v}_+$ is sizable, but it carries only a small magnetization). Hence the faster decay of the $\vec{v}_+$ cannot importantly affect the evolution of the magnetization. What if the heat gradient component is also initially present? Using the estimate $\delta q \sim \frac{m_z}{\chi_s}\delta m_z$ (describing the situation where the magnetic field responsible for δm_z is switched off and excess energy is instantly converted into heat), we find that $\vec{v}_+$ is more prominent in the initial state but still accounts for $\sim 4\%$ of the initial magnetization

modulation. In both cases, the majority of spin diffusion is therefore governed by $D_- \sim D_s$.

VII. CONCLUSIONS

In summary, we calculated the spin Seebeck coefficient in the Hubbard model and discovered a rich behavior with temperature. The spin Seebeck coefficient significantly exceeds the entropic estimate. This occurs due to the unequal scattering of spin minority and spin-majority carriers which give rise to an $\propto m_z U/T$ dependence that adds up to the Heikes' estimate. This is a striking demonstration of the breakdown of the entropic interpretation of the thermopower in a high-temperature regime where *a priori* one would trust it the most. Our predictions for a large spin-thermoelectric effect could be tested on optical lattices. We also calculated the diffusion matrix eigenvalues and estimated the influence of spin thermoelectricity in the existing measurements of the spin diffusion [2]. We found this influence to be moderate and insufficient to explain the discrepancy between the experiment and the theory. Possible directions for future research include simulating explicitly the time dependence in such experiments and the study of possible nonlinear effects.

ACKNOWLEDGMENTS

We acknowledge helpful discussions with Rok Žitko and Antoine Georges. This work was supported by the Slovenian Research Agency (ARRS) under Program No. P1-0044 and Projects No. J1-2458, No. N1-0088, and No. J1-2455-1.

APPENDIX: SPIN TRANSPORT FORMALISM

Here we take advantage of the known general shape of the transport function to obtain an approximate simple expression for the Seebeck coefficient. The temperatures we consider in our simulations (and that pertain to the cold-atom experiments, which motivate our investigation) are large. In Ref. [2] the estimated entropy is 1.1, which pertains to $T \approx 0.3|U|$ (in this Appendix we will phrase the discussion in terms of the attractive Hubbard model), comparable to the bandwidth. Hence the derivative of the Fermi function $df/d\omega$ does not change substantially over each of the Hubbard bands and hence in the transport integrals, Eq. (3), one can approximate the transport function by two $\delta-$ peaks as

$$\Phi(\omega)=\phi_-\delta(\omega - U/2 + \delta\mu) + \phi_+\delta(\omega + U/2 + \delta\mu), \quad \text{(A1)}$$

with different weights ϕ_- and ϕ_+ for the negative and positive frequency peaks, respectively. Note that $U < 0$ in this case. One can evaluate the Seebeck coefficient using this ansatz transport function. Taking also into account that $\delta\mu/T$ is small, one can expand the derivative of the Fermi function, that is, $-df/d\omega(\pm U/2 - \delta\mu) = -df/d\omega(U/2)(1 \pm t_0\delta\mu/T)$, where we define $t_0 = \tanh(U/4T)$. Introducing effective weights (modified from ϕ due to $df/d\omega$) $\tilde{\phi}_\pm = \phi_\pm(1 \mp t_0\delta\mu/T)$, one obtains a simple expression for the Seebeck coefficient

$$S_c = -\frac{U}{2T}\frac{\tilde{\phi}_- - \tilde{\phi}_+}{\tilde{\phi}_- + \tilde{\phi}_+} + \frac{\delta\mu}{T} = S_1 + \frac{\delta\mu}{T}. \quad \text{(A2)}$$

The high-T Seebeck coefficient for the attractive model thus has a Heikes' term (second term of this expression, predicted by Chaikin and Beni [22]) but crucially also the first term, S_1, that is proportional to $U/2T$ and the difference between the effective weights of the peaks of the transport function. Whenever this difference (that, as we discuss next, is due to a different scattering of electrons and holes) does not vanish, the Seebeck coefficient *cannot* be interpreted in terms of the entropic considerations alone. This explains large values of spin Seebeck coefficient seen in numerical results of Fig. 1.

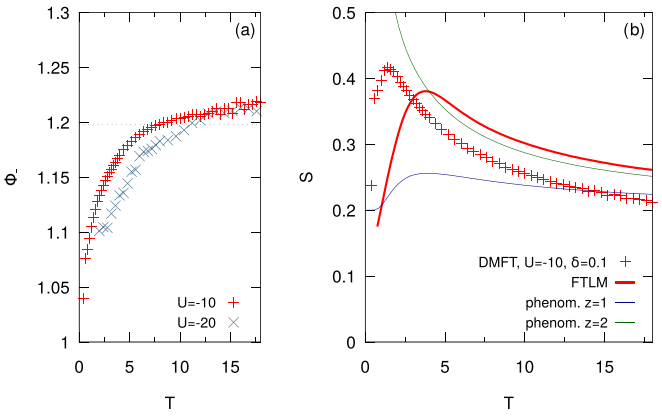

FIG. 4. (a) Weight of the negative frequency peak of transport function ϕ_- for attractive Hubbard model for $\delta = 0.1$ and two values of U. The data are normalized such that total weight $\phi_- + \phi_+ = 2$. The value corresponding to the phenomenological estimate $\phi_- = (1+\delta)^z$ with $z = 2$ is also indicated (dashed). (b) Seebeck coefficient for $U = -10$ compared with estimates based on the assumption of the transport function weights being $\phi_\pm = (1 \mp \delta)^z$ for $z = 1, 2$.

Is scattering really important? Would not the effective weights differ already due to the different weights of the corresponding Hubbard band weights in the density of states? If this were the case, one would have $\phi_\pm \propto (1 \mp \delta)$ (simply from the considerations of occupancy). Incidentally, the influence of $\delta\mu$ just cancels at small T. Namely, for small doping, $\delta\mu/T \approx \delta$. As $T/|U|$ becomes small, $t_0 \to -1$. Hence one has $\tilde{\phi}_\pm \approx \phi_\pm(1 \pm \delta)$ and hence $\tilde{\phi}_+ = \tilde{\phi}_-$. In this limit S_1 would vanish. One needs the to take the scattering into account to understand the occurrence of deviation from entropic estimates.

We plot the weight ϕ_- obtained from the integral of the transport function over negative frequencies normalized such that the total integral is 2 on Fig. 4(a). One sees that in most of the studied temperature range ϕ_- is close to the value expected from the dependence $(1+\delta)^2$. Only at smaller temperatures the weight ϕ_- decreases and actually approaches a smaller value $(1+\delta)$.

In Fig. 4(b) we compare numerical results for S_c with the result of Eq. (A2) where we set $\delta\mu/T$ to the high-temperature Heikes value we approximate the transport function weights with $\phi_\pm \propto (1 \mp \delta)^z$ with $z = 1$ (blue) and with $z = 2$ (green). At small temperatures these lead to a behavior $S_1 = -U/2T(z-1)\delta$ (where corrections of order δ^2 and higher are ignored). For $z = 1$, which corresponds to taking into account just the different number of carriers, S_1 vanishes and the strong increase of S_c seen in numerical simulations is not reproduced. One needs to take into account also different scattering of carriers (as in this approximation embodied for $z = 2$).

[1] P. T. Brown, D. Mitra, E. Guardado-Sanchez, R. Nourafkan, A. Reymbaut, C.-D. Hébert, S. Bergeron, A.-M. S. Tremblay, J. Kokalj, D. A. Huse, P. Schauß, and W. S. Bakr, Bad metallic transport in a cold atom Fermi-Hubbard system, Science **363**, 379 (2019).

[2] M. A. Nichols, L. W. Cheuk, M. Okan, T. R. Hartke, E. Mendez, T. Senthil, E. Khatami, H. Zhang, and M. W. Zwierlein, Spin transport in a Mott insulator of ultracold fermions, Science **363**, 383 (2019).

[3] J. Vučičević, J. Kokalj, R. Žitko, N. Wentzell, D. Tanasković, and J. Mravlje, Conductivity in the Square Lattice Hubbard Model at High Temperatures: Importance of Vertex Corrections, Phys. Rev. Lett. **123**, 036601 (2019).

[4] M. Ulaga, J. Mravlje, and J. Kokalj, Spin diffusion and spin conductivity in the two-dimensional Hubbard model, Phys. Rev. B **103**, 155123 (2021).

[5] I. Žutić, J. Fabian, and S. Das Sarma, Spintronics: Fundamentals and applications, Rev. Mod. Phys. **76**, 323 (2004).

[6] K. Uchida, S. Takahashi, K. Harii, J. Ieda, W. Koshibae, K. Ando, S. Maekawa, and E. Saitoh, Observation of the spin Seebeck effect, Nature (London) **455**, 778 (2008).

[7] H. Adachi, K. Uchida, E. Saitoh, and S. Maekawa, Theory of the spin Seebeck effect, Rep. Prog. Phys. **76**, 036501 (2013).

[8] D. Hirobe, M. Sato, T. Kawamata, Y. Shiomi, K. Uchida, R. Iguchi, Y. Koike, S. Maekawa, and E. Saitoh, One-dimensional spinon spin currents, Nat. Phys. **13**, 30 (2017).

[9] T. W. Silk, I. Terasaki, T. Fujii, and A. J. Schofield, Out-of-plane thermopower of strongly correlated layered systems: An application to $Bi_2(Sr, La)_2CaCu_2O_{8+\delta}$, Phys. Rev. B **79**, 134527 (2009).

[10] M. R. Peterson and B. S. Shastry, Kelvin formula for thermopower, Phys. Rev. B **82**, 195105 (2010).

[11] X. Deng, J. Mravlje, R. Žitko, M. Ferrero, G. Kotliar, and A. Georges, How Bad Metals Turn Good: Spectroscopic Signatures of Resilient Quasiparticles, Phys. Rev. Lett. **110**, 086401 (2013).

[12] J. Kokalj and R. H. McKenzie, Enhancement of the thermoelectric power by electronic correlations in bad metals: A study of the Kelvin formula, Phys. Rev. B **91**, 125143 (2015).

[13] J. Mravlje and A. Georges, Thermopower and Entropy: Lessons from Sr_2RuO_4, Phys. Rev. Lett. **117**, 036401 (2016).

[14] V. J. Emery, Theory of the quasi-one-dimensional electron gas with strong "on-site" interactions, Phys. Rev. B **14**, 2989 (1976).

[15] L. Laloux, A. Georges, and W. Krauth, Effect of a magnetic field on Mott-Hubbard systems, Phys. Rev. B **50**, 3092 (1994).

[16] M. Keller, W. Metzner, and U. Schollwöck, Dynamical Mean-Field Theory for Pairing and Spin Gap in the Attractive Hubbard Model, Phys. Rev. Lett. **86**, 4612 (2001).

[17] M. Capone, C. Castellani, and M. Grilli, First-Order Pairing Transition and Single-Particle Spectral Function in the Attractive Hubbard Model, Phys. Rev. Lett. **88**, 126403 (2002).

[18] A. Toschi, P. Barone, M. Capone, and C. Castellani, Pairing and superconductivity from weak to strong coupling in the attractive Hubbard model, New J. Phys. **7**, 7 (2005).

[19] A. Moreo and D. J. Scalapino, Cold Attractive Spin Polarized Fermi Lattice Gases and the Doped Positive U Hubbard Model, Phys. Rev. Lett. **98**, 216402 (2007).

[20] N. A. Kuleeva, E. Z. Kuchinskii, and M. V. Sadovskii, Normal phase and superconducting instability in the attractive Hubbard model: a DMFT(NRG) study, J. Exp. Theor. Phys. **119**, 264 (2014).

[21] R. Žitko, Ž. Osolin, and P. Jeglič, Repulsive versus attractive Hubbard model: Transport properties and spin-lattice relaxation rate, Phys. Rev. B **91**, 155111 (2015).

[22] P. M. Chaikin and G. Beni, Thermopower in the correlated hopping regime, Phys. Rev. B **13**, 647 (1976).

[23] J. Jaklič and P. Prelovšek, Finite-temperature properties of doped antiferromagnets, Adv. Phys. **49**, 1 (2000).

[24] P. Prelovšek and J. Bonča, in *Strongly Correlated Systems: Numerical Methods*, edited by A. Avella and F. Mancini, Springer Series in Solid-State Sciences (Springer Berlin Heidelberg, 2013), pp. 1–30.

[25] J. Kokalj and R. H. McKenzie, Thermodynamics of a Bad Metal-Mott Insulator Transition in the Presence of Frustration, Phys. Rev. Lett. **110**, 206402 (2013).

[26] A. Georges, G. Kotliar, W. Krauth, and M. J. Rozenberg, Dynamical mean-field theory of strongly correlated fermion systems and the limit of infinite dimensions, Rev. Mod. Phys. **68**, 13 (1996).

[27] R. Bulla, T. A. Costi, and T. Pruschke, Numerical renormalization group method for quantum impurity systems, Rev. Mod. Phys. **80**, 395 (2008).

[28] R. Žitko and T. Pruschke, Energy resolution and discretization artifacts in the numerical renormalization group, Phys. Rev. B **79**, 085106 (2009).

[29] G. Palsson and G. Kotliar, Thermoelectric Response Near the Density Driven Mott Transition, Phys. Rev. Lett. **80**, 4775 (1998).

[30] B. Kyung and A. M. S. Tremblay, Mott Transition, Antiferromagnetism, and d-Wave Superconductivity in Two-Dimensional Organic Conductors, Phys. Rev. Lett. **97**, 046402 (2006).

[31] A. Georges and J. Mravlje, Skewed non-Fermi liquids and the Seebeck effect, Phys. Rev. Res. **3**, 043132 (2021).

[32] A. Gourgout, G. Grissonnanche, F. Laliberté, A. Ataei, L. Chen, S. Verret, J.-S. Zhou, J. Mravlje, A. Georges, N. Doiron-Leyraud, and L. Taillefer, Seebeck Coefficient in a Cuprate Superconductor: Particle-Hole Asymmetry in the Strange Metal Phase and Fermi Surface Transformation in the Pseudogap Phase, Phys. Rev. X **12**, 011037 (2022).

[33] S. A. Hartnoll, Theory of universal incoherent metallic transport, Nat. Phys. **11**, 54 (2015).

[34] Notice that we are considering an undoped, particle-hole symmetric case; hence the charge thermoelectric effect vanishes and the Nernst-Einstein equation is given in terms of 2×2 matrices. Away from particle-hole symmetry charge transport effects would need to be considered as well and diffusion would be given in terms of 3×3 matrices.